Properties of the second-order nonlinear optical susceptibility $\chi^{(2)}$ in asymmetric undoped AlGaAs/InGaAs double quantum wells

Tae-ik Park, Godfrey Gumbs,[a),b)] and Y. C. Chen[a)]
Department of Physics and Astronomy, Hunter College of the City University of New York, 695 Park Avenue, New York, New York 10021

(Received 2 November 1998; accepted for publication 17 April 1999)

The second-order nonlinear optical susceptibility $\chi^{(2)}$ for second-harmonic generation is calculated for the 11H transition of a graded double quantum well (DQW) structure of undoped $GaAs/Al_xGa_{1-x}As$. These results are compared with the single quantum well (QW). Our results show that the values of $\chi^{(2)}$ have optimal magnitudes dependent on the width, depth and separation between the QWs in a DQW structure. When the electric field increases, the dipole moment increases due to the increasing separation between the electron and hole wave functions. On the other hand, the oscillator strength of the 11H transition is reduced as a result of the decrease in the overlap of the electron and hole envelope functions. These two competing factors give rise to optimal conditions for the enhancement of the second-order nonlinear susceptibility $\chi^{(2)}$. It is demonstrated that $\chi^{(2)}$ for the DQW structure is more enhanced than for the biased single QW. © *1999 American Institute of Physics.* [S0021-8979(99)01215-3]

I. INTRODUCTION

Since the discovery of second-harmonic generation (SHG) by Franken *et al.* in 1961, shortly after the demonstration of the first working laser by Maiman in 1960, nonlinear optics has received a considerable amount of attention over the years.[1] The nonlinear optical response has been mainly described by $\chi^{(2)}$ (the second-order nonlinear optical susceptibility) and $\chi^{(3)}$ (the third-order nonlinear optical susceptibility) even though higher order effects may be significant. $\chi^{(2)}$ has its own characteristics in that it has nonzero values for the noncentrosymmetric crystals that do not display inversion symmetry. On the other hand, $\chi^{(3)}$ has its own characteristics in that this function can have nonzero values both for centrosymmetric and noncentrosymmetric media. In particular, second-order effects such as frequency mixing including SHG, sum (and difference) frequency generation (SFG and DFG) and linear electro-optic (Pockels) effect are of great practical interest in the areas of integrated optics and optical communications. The large value of $\chi^{(2)}$ can lead to the miniaturization of efficient optical devices such as frequency-tunable visible lasers (using SFG) and optical parametric oscillators (using DFG).[1] So far, many papers dealing with the enhancement of $\chi^{(2)}$ for an asymmetric quantum well (QW), asymmetric double quantum well (DQW) and other structures (e.g., bond-alternating dipolar structures) have been published.[2–8] In these papers, large values of $\chi^{(2)}$ were obtained under suitable conditions. Typically, the magnitude of $\chi^{(2)}$ is of order 5×10^{-8} cm/statvolt or $\sim1.67\times10^{-12}$ m/V. However, In Refs. 2–8, $\chi^{(2)}$ is enhanced by 2 orders of magnitude. In addition to these works, many papers dealing with calculation of $\chi^{(2)}$ for a single QW biased by an electric field have also been published.[9–12] In Ref. 9, Kuwatsuka and Ishikawa clearly discuss the properties of $\chi^{(2)}$. As the electric field increases, the dipole moment increases due to the separation of the electron and hole overlap wave functions, while the oscillator strength weakens due to the decrease of the overlap integral of the electron and hole envelope functions. Therefore, an optimum electric field exists for each well width. A value for $\chi^{(2)}$ of more than 5×10^{-10} m/V (which is the $\chi^{(2)}$ value of bulk GaAs) was obtained for a 70 Å well width with an electric field of 1.5×10^{7} V/m.[9] In our paper, we present results for $\chi^{(2)}$ for various asymmetric well structures. From a theoretical point of view, the nonlinear effects depend on the origin of coordinates along the growth direction of the QW structure since the polarization is defined in terms of a dipolar displacement of charge. In particular, for an asymmetric QW structure, a careful choice of the origin must be made since, for example, if there are several subbands occupied, each subband level has a different charge distribution. Some papers take the geometrical origin on the left-hand side of the QW.[3,7] Some others choose the origin at the center of the well,[4,5] while it is not clear where others have chosen their origin of coordinates.[2] As far as we know, there has not been a clear statement concerning the origin of coordinates in the calculation of $\chi^{(2)}$ for QWs. In this paper, we present numerical results for $\chi^{(2)}$ for transitions between the first conduction and first heavy hole subbands of an asymmetric intrinsic AlGaAs/InGaAs double quantum well.

II. THEORY

We consider an intrinsic DQW structure with finite width along the z axis which is the direction of confinement (i.e., subband quantization) as shown in Fig. 1. In the absence of doping, the Schrödinger equation for an electron of charge $-e$ in a uniform electric field E is given by

[a)]Also at: The Graduate School and University Center of the City University of New York, 33 West 42 Street, New York, NY 10036.
[b)]Electronic mail: gumbs@apollo.ph.hunter.cuny.edu

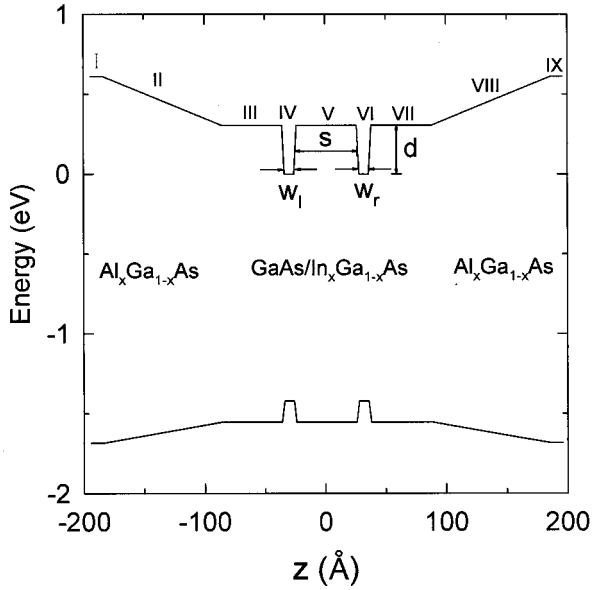

FIG. 1. Band edge for a double quantum well GRINSCH structure. Regions I and IX consist of $Al_{0.6}Ga_{0.4}As$, regions III, V and VII consist of $Al_{0.3}Ga_{0.7}As$. The left QW (region IV) is fixed as GaAs with a width of 10 Å and a depth of 0.284 eV in the conduction band and a depth of 0.153 eV in the valence band. The QW on the right-hand side consists of $In_xGa_{1-x}As$ whose depth d depends on the In composition x.

$$\left\{-\frac{\hbar^2}{2m^*_{(c,v)}(z)}\left(\frac{\partial^2}{\partial x^2}+\frac{\partial^2}{\partial y^2}\right)-\frac{\hbar^2}{2}\frac{\partial}{\partial z}\frac{1}{m^*_{(c,v)}(z)}\frac{\partial}{\partial z}+V_{(c,v)b}(z)-eEz\right\}\Psi_{(c,v)}(\mathbf{r})=\epsilon\Psi_{(c,v)}(\mathbf{r}), \tag{1}$$

where the subscripts c and v denote the conduction and valence band, respectively, $m^*_{(c,v)}(z)$ is the z-dependent electron effective mass in the conduction band or the hole effective mass in the valence band, and $V_{(c,v)b}(z)$ is the band edge of the conduction or valence band. The total wave function $\Psi(\mathbf{r})$ is

$$\Psi_{(c,v)}(\mathbf{x}_\parallel,z)=u_{(c,v)}(\mathbf{x}_\parallel)e^{i\mathbf{k}_\parallel\cdot\mathbf{x}_\parallel}\phi_{(c,v),n}(z), \tag{2}$$

where $u_{(c,v)}(\mathbf{x}_\parallel)$ is the normalized Bloch function of the conduction or valence band, $\mathbf{x}_\parallel$ is the 2D position vector and $\mathbf{k}_\parallel$ is the 2D wave vector of an electron in the plane of the QW, respectively. The normalized envelope wave function of the bound states $\phi_n(z)$ satisfies the following 1D Schrödinger equation:

$$\left\{-\frac{\hbar^2}{2}\frac{\partial}{\partial z}\frac{1}{m^*_{(c,v),n}(z)}\frac{\partial}{\partial z}+V_{(c,v),b}(z)-eEz\right\}\phi_{(c,v),n}(z)=\epsilon_{(c,v),n}\phi_{(c,v),n}(z), \tag{3}$$

where, $\epsilon_{(c,v),n}$ is the nth subband energy in the conduction and valence band.

Making use of these eigenfunctions and eigenvalues, one can calculate $\chi^{(2)}$ numerically, obtained through the density matrix formalism of quantum mechanics. This formalism is suitable because it is capable of treating effects due to temperature and impurity scattering. It is well known that for an electron density equal to N, the nonlinear optical susceptibility $\chi^{(2)}_{ijk}$ is given by (see, for example, Sec. 3.6 of Ref. 1 and Ref. 13; i,j,k represent x,y,z)

$$\begin{aligned}\chi^{(2)}_{ijk}(\omega)=-N\frac{e^3}{\hbar^2}\sum_{gnn'}\Bigg\{&\frac{(r_i)_{gn}(r_j)_{nn'}(r_k)_{n'g}}{(\omega-\omega_{ng}+i\Gamma_{ng})(\omega_2-\omega_{n'g}+i\Gamma_{n'g})}+\frac{(r_i)_{gn}(r_k)_{nn'}(r_j)_{n'g}}{(\omega-\omega_{ng}+i\Gamma_{ng})(\omega_1-\omega_{n'g}+i\Gamma_{n'g})}\\&+\frac{(r_k)_{gn'}(r_j)_{n'n}(r_i)_{ng}}{(\omega+\omega_{ng}+i\Gamma_{ng})(\omega_2+\omega_{n'g}+i\Gamma_{n'g})}+\frac{(r_j)_{gn'}(r_k)_{n'n}(r_i)_{ng}}{(\omega+\omega_{ng}+i\Gamma_{ng})(\omega_1+\omega_{n'g}+i\Gamma_{n'g})}\\&-\frac{(r_j)_{ng}(r_i)_{n'n}(r_k)_{gn'}}{\omega-\omega_{nn'}+i\Gamma_{nn'}}\left(\frac{1}{\omega_2+\omega_{n'g}+i\Gamma_{n'g}}+\frac{1}{\omega_1-\omega_{ng}+i\Gamma_{ng}}\right)-\frac{(r_k)_{ng}(r_i)_{n'n}(r_j)_{gn'}}{\omega-\omega_{nn'}+i\Gamma_{nn'}}\\&\times\left(\frac{1}{\omega_2-\omega_{ng}+i\Gamma_{ng}}+\frac{1}{\omega_1+\omega_{n'g}+i\Gamma_{n'g}}\right)\Bigg\}\rho^{(0)}_g.\end{aligned} \tag{4}$$

For solids, the eigenfunctions are given by Eq. (2) and $\rho^{(0)}_g$ denotes the Fermi-Dirac distribution function. Also, $(r_i)_{n'n}$ is a dipole matrix element between energy eigenstates, $\hbar\omega_{nn'}$ is the $\mathbf{k}_\parallel$ dependent transition energy between energy eigenstates and $\Gamma_{nn'}$ is an inverse relaxation time. Consequently, Eq. (4) can be expressed in terms of the Bloch states $u_{(c,v)}(\mathbf{x}_\parallel)$ and the envelope function $\phi_{(c,v),n}(z)$. We assume that the materials making up the heterojunction are direct gap semiconductors. This is true for $GaAs/Al_xGa_{1-x}As$ for the alloy composition $x<0.42$ with both the valence band maximum and the conduction band minimum at the Γ point.[14] We restrict our attention to a calculation of $\chi^{(2)}_{zxy}$ which is given by

$$\begin{aligned}\chi^{(2)}_{zxy}(2\omega=\omega+\omega)=-\frac{2e^3}{\epsilon_0\hbar^2}\int d^2\mathbf{k}_\parallel\sum_{lmn}f^v_l(\mathbf{k}_\parallel)&\times\langle u_v|x|u_c\rangle\langle u_v|y|u_c\rangle\\&\times\frac{\langle\phi^v_l|\phi^c_m\rangle\langle\phi^c_m|z|\phi^c_n\rangle\langle\phi^c_n|\phi^v_l\rangle}{(\omega-(\omega^c_m-\omega^v_l)+i\Gamma)(\omega+(\omega^c_n-\omega^v_l)+i\Gamma)},\end{aligned} \tag{5}$$

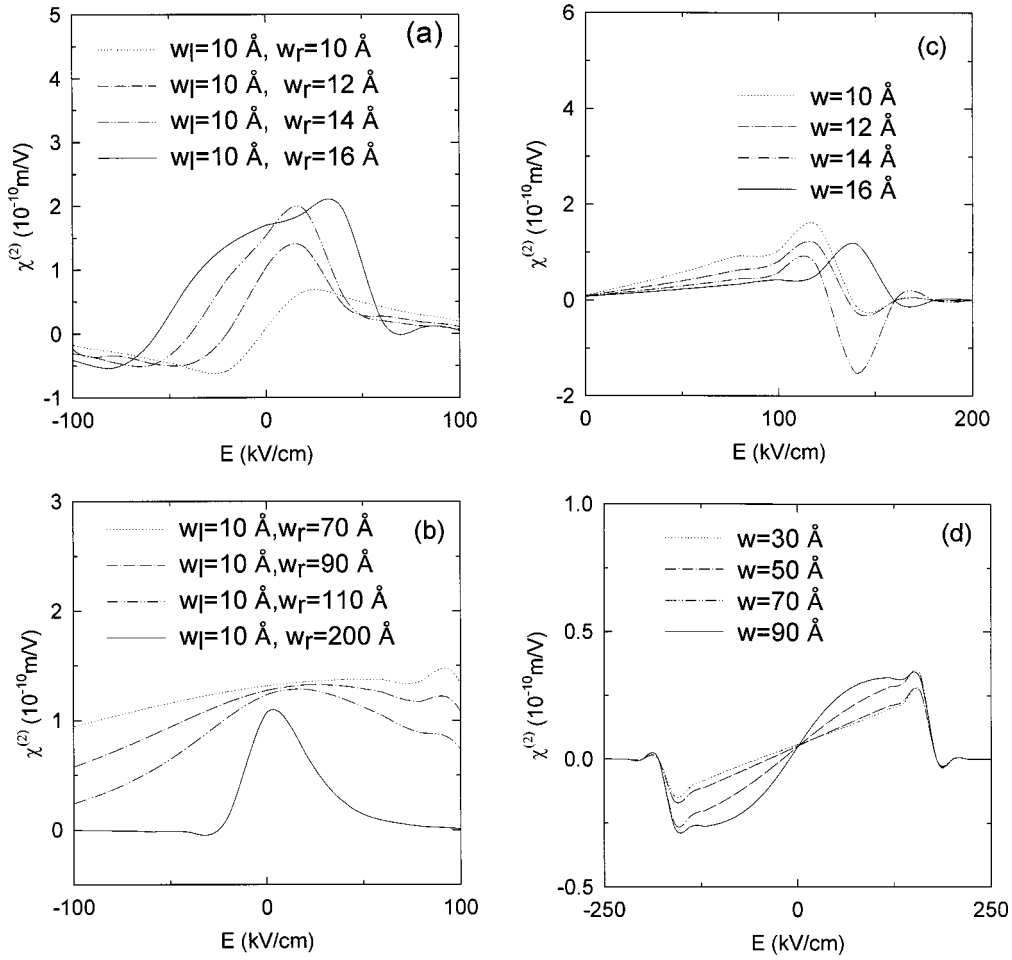

FIG. 2. Plots of $\chi^{(2)}_{zxy}$ as a function of electric field, for a frequency equal to half the band gap. In (a) and (b), the DQW structure has a well on the right of different width w_r chosen as shown but with fixed width $w_l = 10$ Å for the well on the left. The material for each QW is GaAs whose well depth is $d = 0.284$ eV for the conduction band and $d = 0.153$ eV for the valence band. The separation between the wells is $s = 52$ Å. In (c) and (d), there is a single GaAs square QW with the same depth as the DQW structure.

where we have assumed that the impurity scattering is independent of the subband index. In our calculations, we used $\Gamma = 10^{12}\,\mathrm{s}^{-1}$. Also, in this notation, $f^{v}_{l}(\mathbf{k}_{\|})$ denotes the Fermi-Dirac distribution function for electrons in the valence band.

III. NUMERICAL RESULTS AND DISCUSSION

In this section, we present numerical results for $\chi^{(2)}_{zxy}$. As shown in Fig. 1, the DQW structure is divided into nine regions for a graded index of refraction separate confinement heterostructure (GRINSCH). Regions I and IX consist of $Al_{0.6}Ga_{0.4}As$ of thickness 10 Å, regions III, VII (each of thickness 50 Å), and region V consist of $Al_{0.3}Ga_{0.7}As$, whereas II and VIII are graded and of thickness 100 Å.[15] The left QW (LQW) forming region IV is fixed as GaAs of width 10 Å and a depth of 0.284 eV in the conduction band and 0.153 eV in the valence band. For zero electric field, there are only two subband levels in either the conduction or the valence band (with energy levels $\epsilon_{c,1} = 0.235$, $\epsilon_{c,2} = 0.262$, $\epsilon_{v,1} = 0.113$, and $\epsilon_{v,2} = 0.117$). Therefore, the second energy level is barely confined to in the well and can thus be removed by applying an external electric field. On the other hand, the right QW (RQW) shown as region VI, is composed of $In_xGa_{1-x}As$ so that we can change the depth of the well. Accordingly, an asymmetric DQW structure is achieved by varying the width w_r of the RQW, its depth d, and the distance s between the LQW and the RQW. Here, we use an intrinsic GaAs/InGaAs DQW structure in which an electron makes a transition between the first conduction and first heavy hole (11H). Since we restrict our attention to the 11H transition, we can set the origin of coordinates along the z direction to be the center of the charge distribution for the first heavy hole subband.

A. GaAs/GaAs DQW

We now present numerical results in Figs. 2(a) and 2(b) for $\chi^{(2)}$ for a DQW with GaAs forming the LQW and GaAs forming the RQW. The widths of the two wells are chosen unequal to make the system asymmetric. In Fig. 2(a), the width of the LQW is fixed as 10 Å and the width of the RQW is chosen successively as 10, 12, 14, and 16 Å with the same depth d and separation $s = 52$ Å. When both wells have a width of 10 Å [dotted line in Fig. 2(a)], $\chi^{(2)}_{zxy}$ is antisymmetric about zero electric field. The magnitude of $\chi^{(2)}$ is drastically increased as soon as the width of the RQW is changed to 12 Å, thereby breaking the symmetry of the DQW. With this small change in width, most of the charge

distribution is shifted to one side.[16] So that a polarization of the charge is abruptly generated and the value of $\chi^{(2)}$ is increased at zero electric field. As the width of the RQW is increased, the polarization charge is more separated and the magnitude of $\chi^{(2)}$ is increased. Figure 2(b) shows that for the wider QWs from 70 to 130 Å, the effect due to increasing the well width is reversed. When the well width is increased from 10 to 16 Å, the electric field $E_{\max}$ which gives the largest $\chi^{(2)}$ is increased, but $E_{\max}$ is decreased when the well width is increased from 70 to 130 Å. Therefore, there is an optimal electric field and well width determining the largest $\chi^{(2)}$. This result can be understood as a competition between the dipolar effect and the oscillator strength for the optical transition. Clearly, from Eq. (5) as the electric field increases, the dipole moment increases due to the increase in separation between the electron and hole eigenfunctions. However, the oscillator strength is weakened due to a decrease in the overlap integral of the electron and hole envelope functions. Therefore, it is expected that optimum conditions will be achieved for some value of the electric field and well width. From a physical point of view, if one QW is much wider than the other, the limiting case for a single square well will be obtained and the value for $\chi^{(2)}$ will be decreased. Furthermore, when the well width is increased from 10 to 16 Å, the response range of the electric field is increased. This can be understood as follows: when an electric field is applied, the band edge is tilted and less charge can be confined to the QW. But, if the well width is increased, more charge can be contained in the well leading to a wider response range of the electric field (range of finite values for $\chi^{(2)}$), as shown in Fig. 2(a). Also, the fact that $\chi^{(2)}$ is flat in this range means that the system is not very sensitive to a change in the electric field over this range. However, for very wide QWs, the range of response for the electric field can be reduced with increasing QW width, as shown in Fig. 2(b). The reason for this is that when the band edge is tilted by a chosen electric field, the electron wave function has a larger change in shape within the wider QW and the electron charge can be depleted in the well, i.e., there is less confinement of the electrons. Consequently, the response to the electric field takes place over a narrower range for the wider QW. Similar results are obtained for single QWs as we show in Figs. 2(c) and 2(d). The results in Fig. 2(d) agree with previously published calculations in Ref. 9. The difference is in Fig. 2(c) where the effect is reversed for very narrow QWs (widths less than 30 Å). The key difference is that $\chi^{(2)}_{zxy}$ for DQWs has larger peak values than for single QWs. Figure 2(c) shows that as the well width is increased, the slope near $E=0$ is decreased. Also, near $E=150\,\mathrm{kV/cm}$, an abrupt change takes place. This is due to the displacement of the charge from the well. The narrower the well width, the higher is the subband energy level. Therefore, when the well is tilted by the applied electric field, the electronic charge distribution close to the top of the well spills out leading to a sharp drop in $\chi^{(2)}$. In Fig. 2(d), the well widths are larger than in Fig. 2(c) and that is why there is no abrupt drop of the magnitude near $E=150\,\mathrm{kV/cm}$. Furthermore, in contrast to the narrow well case, when the width of the well is increased, the slope is increased. The reason for this is because the larger the well width, the greater the amount of charge that can be located in the well, so that when the well is tilted by an electric field, the dipole effect is more likely due to the increased separation. This is why when the width of the well is increased, the slope of $\chi^{(2)}$ is increased.

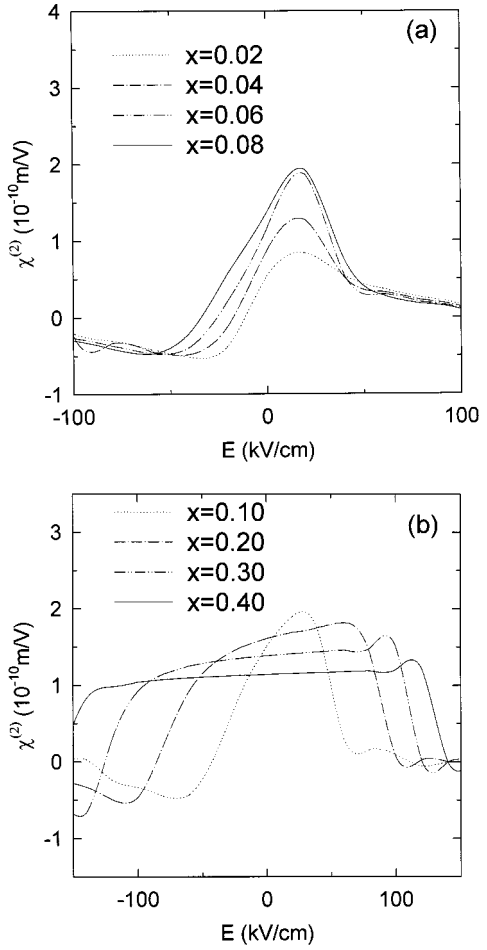

FIG. 3. Plots of $\chi^{(2)}_{zxy}$ as a function of a constant external electric field. The left QW is GaAs of width $w_l=10$ Å and band offset $d=0.284$ eV for the conduction band and $d=0.153$ eV for the valence band. The right QW is $In_xGa_{1-x}As$ and the separation between the wells is chosen as $s=52$ Å. Results are presented for a range of In composition with $0.02\leqslant x\leqslant 0.08$ in (a) and $0.10\leqslant x\leqslant 0.30$ in (b).

B. GaAs/InGaAs DQW

In Fig. 3, we present numerical results for a DQW with GaAs forming the left QW and $In_xGa_{1-x}As$ forming the QW on the right. The width of these two wells is fixed at 10 Å and the separation between them is chosen as $s=52$ Å. The structure is made asymmetric by changing the In composition. When x is increased, the depth d of the right QW is increased. As a matter of fact, when x is increased from 0.02 to 0.08, the peak height of $\chi^{(2)}_{zxy}$ increases monotonically, as shown in Fig. 3(a), because the polarization increases with the degree of asymmetry within the structure. Figure 3(b) presents results for $\chi^{(2)}_{zxy}$ for larger x values. When the right QW is much deeper than the one on the left, most of the charge distribution is shifted to the right QW and $\chi^{(2)}$ be-

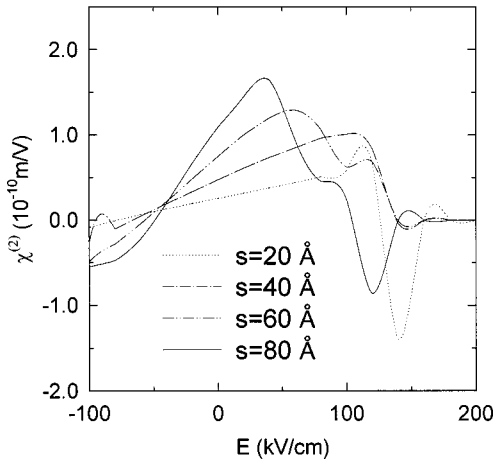

FIG. 4. Results for $\chi^{(2)}_{zxy}$ of a DQW as a function of the electric field for various separations s between the QW on the left made up GaAs and the QW on the right consisting of $In_{0.1}Ga_{0.9}As$ DQW. The left QW has width $w_l = 10$ Å and band offset $d = 0.284$ eV for the conduction band and $d = 0.153$ eV for the valence band. The right QW is $In_{0.1}Ga_{0.9}As$. The separation s is varied from 20 to 80 Å.

haves like that for a single QW. The abrupt decrease seen near the high electric field $E = 100$kV/cm in Fig. 3(b) is also due to the lack of confinement by the well as the electrons spill over the top.

Figure 4 shows the behavior of $\chi^{(2)}_{zxy}$ for various values of the barrier width s between the two wells of a DQW system with $20\,\text{Å} \leqslant s \leqslant 80\,\text{Å}$. In these calculations, the widths of the left and right QWs, w_l and w_r, respectively, were equal and fixed with the LQW consisting of GaAs and the RQW is $In_{0.1}Ga_{0.9}As$. When s is increased, the magnitude of $\chi^{(2)}_{zxy}$ is increased due to the increased polarization produced by the larger separation between the electron and hole charge distributions. Figure 4 has the largest value of $\chi^{(2)}_{zxy}$ compared with the results in Figs. 2 and 3 due to the asymmetry caused by both the difference in well depths and the large separation between the wells. By increasing the separation between the QWs. the magnitude will continue to increase but the drawback from a practical point of view is that the response range of the electric field becomes very narrow.

IV. CONCLUDING REMARKS

In summary, we have calculated $\chi^{(2)}_{zxy}$ for second-harmonic generation for the 11H transition of a GRINSCH double QW structure of undoped $GaAs/Al_xGa_{1-x}As$. We chose the origin of coordinates along the growth direction as the center of the charge distribution of the first heavy hole in the valence band. Our results show that the values of $\chi^{(2)}$ have optimal values dependent on the width, depth and separation between the QWs in a DQW structure. When the electric field increases, the dipole moment increases due to the increasing separation between the electron and hole wave functions. On the other hand, the oscillator strength of the 11H transition is reduced as a result of the decrease in the overlap of the electron and hole envelope functions. These two competing factors may give rise to optimal conditions for the enhancement of the second order nonlinear susceptibility $\chi^{(2)}$. Increasing the separation between the QWs also increases the maximum value that $\chi^{(2)}$ can have but the response takes place over a reduced range of electric fields. We have demonstrated that $\chi^{(2)}$ for the DQW GRINSCH structure is more enhanced than for the biased single QW. Also, because the barrier regions where the graded structure are far from the QWs, we do not expect that removing the graded regions will result in any significant change in our conclusions.

ACKNOWLEDGMENTS

The authors G.G. and T.P. acknowledge the support in part from the National Science Foundation Grant No. INT-9402741 (U.S.—U.K. Collaborative Grant), the City University of New York PSC-CUNY Grant No. 664279, as well as the Minority Biomedical Research Support (MBRS) Grant No. GM56945-01 from the NIH. Y.C.C. is supported by the New York State Center for Advanced Technology on Ultrafast Photonic Materials and Applications at the City University of New York.

[1] For a review, see R. W. Boyd, *Nonlinear Optics* (Academic, New York, 1992).
[2] J. Khurgin, Appl. Phys. Lett. **51**, 2100 (1987).
[3] E. Rosencher, P. Bois, J. Nagle, E. Costard, and S. Delaite, Appl. Phys. Lett. **55**, 1597 (1989).
[4] S. J. B. Yoo, M. M. Fejer, R. L. Byer, and J. S. Harris, Jr., Appl. Phys. Lett. **58**, 1724 (1991).
[5] P. J. Harshman and S. Wang, Appl. Phys. Lett. **60**, 1277 (1992).
[6] M. J. Shaw, K. B. Wong, and M. Jaros, Phys. Rev. B **48**, 2001 (1993).
[7] M. Seto *et al.*, Appl. Phys. Lett. **65**, 2969 (1994).
[8] Y. M. Cai, S. Yamada, O. Zamani-Khamiri, A. P. Garito, and K. Y. Wong, Phys. Rev. B **55**, 12985 (1997).
[9] H. Kuwatsuka and H. Ishikawa, Phys. Rev. B **50**, 5323 (1994).
[10] L. Tsang, D. Ahn, and S. L. Chuang, Appl. Phys. Lett. **52**, 697 (1988).
[11] M. M. Fejer, S. J. B. Yoo, R. L. Byer, A. Harwitt, and J. S. Harris, Jr., Phys. Rev. Lett. **62**, 1041 (1989).
[12] L. C. West and S. J. Eglash, Appl. Phys. Lett. **46**, 1156 (1985).
[13] For a derivation of Eq. (4), see Y. R. Shen, *The Principles of Nonlinear Optics* (Wiley, New York, 1984).
[14] R. Enderlein and N. J. M. Horing, *Fundamentals of Semiconductor Physics and Devices* (World Scientific, Singapore, 1997), Sec. 3.7.
[15] For $In_xGa_{1-x}As$, the energy gap E_g (in eV) is $1.422 - 1.53x + 0.45x^2$; for $Al_xGa_{1-x}As$, the energy gap (in eV) is $1.422(1-x) + 2.677x$. The band offset for the conduction band is taken to be $\Delta E_c = 0.70\Delta E_g$ and $\Delta E_v = 0.30\Delta E_g$ for the valence band, where ΔE_g is the discontinuity of the energy gap for the two bulk materials forming the adjacent layers.
[16] L. Lang and K. Nish, Appl. Phys. Lett. **45**, 98 (1984).